Commun. Comput. Phys.
doi: 10.4208/cicp.030311.230911a

Vol. **12**, No. 4, pp. 1033-1050
October 2012

A New Approach to Implement Sigma Coordinate in a Numerical Model

Yiyuan Li[1], Donghai Wang[2,*] and Bin Wang[1,3]

[1] *State Key Laboratory of Numerical Modeling for Atmospheric Sciences and Geophysical Fluid Dynamics, Institute of Atmospheric Physics, Chinese Academy of Sciences, Beijing, China.*
[2] *State Key Laboratory of Severe Weather, Chinese Academy of Meteorological Sciences, Beijing, China.*
[3] *Ministry of Education Key Laboratory for Earth System Modeling, and Center for Earth System Science, Tsinghua University, Beijing, China.*

Received 3 March 2011; Accepted (in revised version) 23 September 2011

Communicated by Lianjie Huang

Available online 28 March 2012

Abstract. This study shows a new way to implement terrain-following σ-coordinate in a numerical model, which does not lead to the well-known "pressure gradient force (PGF)" problem. First, the causes of the PGF problem are analyzed with existing methods that are categorized into two different types based on the causes. Then, the new method that bypasses the PGF problem all together is proposed. By comparing these three methods and analyzing the expression of the scalar gradient in a curvilinear coordinate system, this study finds out that only when using the covariant scalar equations of σ-coordinate will the PGF computational form have one term in each momentum component equation, thereby avoiding the PGF problem completely. A convenient way of implementing the covariant scalar equations of σ-coordinate in a numerical atmospheric model is illustrated, which is to set corresponding parameters in the scalar equations of the Cartesian coordinate. Finally, two idealized experiments manifest that the PGF calculated with the new method is more accurate than using the classic one. This method can be used for oceanic models as well, and needs to be tested in both the atmospheric and oceanic models.

AMS subject classifications: 86-08, 86A05, 86A10

Key words: Pressure gradient force (PGF), terrain-following sigma coordinate, non-orthogonal, basis vectors, numerical modeling, computational errors.

*Corresponding author. *Email addresses:* liyiyuan@mail.iap.ac.cn (Y. Li), d.wang@hotmail.com (D. Wang), wab@lasg.iap.ac.cn (B. Wang)

1 Introduction

A terrain-following σ-coordinate is preferred in both atmospheric and oceanic models, due to its benefit of implementing boundary conditions, the concept of which was initiated by Phillips [1]. There are, however, some disadvantages associated with σ-coordinate, among which the most concerned one is the computational error associated with pressure gradient force (PGF), resulted from the computational form of PGF in σ-coordinate that has more than one term [2,3]. The PGF problem was first pointed out by Smagorinsky et al. [4].

As horizontal resolutions of numerical models increase, the PGF problem becomes more critical [5, 6]. A common view is that the PGF problem is caused by using σ-coordinate, and a number of methods have been designed to overcome this problem mostly via adjusting model parameters or constructing different algorithms for PGF terms. Corby et al. [7] was the first to design a finite difference scheme for PGF, and Gary [8] proposed to subtract reference state of density profile before calculating PGF. Qian and Zhong [9] introduced a general difference scheme for PGF focusing on the coordinate transformation near terrain. More complicated methods were subsequently proposed, such as the Jacobian method by Blumberg and Mellor [10] and the high-order schemes by McCalpin [11]. More recently, a recurrent computational methods of PGF based on hydrostatic equilibrium was proposed by Yang and Qian [12], a linear programming procedure was proposed by Sikirić et al. [13], and a perfectly balanced method for estimating PGF was suggested by Berntsen [14]. Note that all these existing methods are designed to alleviate the errors to an acceptable level, after the PGF computational form has already had more than one term. As few researches about how the problem started at the first place has been done, we try to adopt a completely new approach here, with which we obtain a set of equations in σ-coordinate that has only one term in the computational form of the PGF. In another word, we bypass the PGF problem all together.

In this study, we first explain why the PGF computational form in σ-coordinate has more than one term by means of classifying the existing methods using σ-coordinate and analyzing the expression of the scalar gradient in a curvilinear coordinate system. Based on these analyses, we elucidate that using the covariant scalar equations of σ-coordinate in a numerical model can avoid the PGF problem all together, while the simple form of boundary conditions is preserved. Finally, via two idealized experiments, we validate that the new method can calculate the PGF more precisely.

2 Analysis of the PGF problem

Many scholars have analyzed the PGF problem in σ-coordinate, and concluded that the source of the problem is the computational form of PGF being expanded into two parts. The same problem can be caused by two different ways, as we show in the later part through classifying the existing methods.

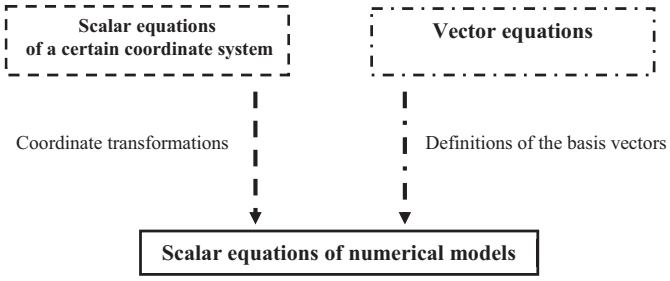

Figure 1: A schematic of two different ways of obtaining scalar equations in numerical models.

2.1 Methods of using σ-coordinate

To use σ-coordinate in a numerical model is basically to choose a set of equations. The methods of obtaining the scalar equations in a numerical model can be classified into two types (Fig. 1): the first type is to transform the scalar equations from one coordinate system to another, and the other type is to expand vector equations to scalar equations of the same coordinate. Specifically, the first type is to use coordinate transformation relations, called the chain rule, to obtain the relations of spatial partial derivatives between two different coordinates. As a result, the scalar equations of one coordinate system are transformed to another. The other type is to expand vector equations into scalar equations according to the basis vectors of some coordinate, and then to obtain the scalar equations of the same coordinate.

Most numerical models use the first type to obtain basis scalar equations, including the Regional Atmospheric Modeling System (RAMS), the Coupled Ocean/Atmosphere Mesoscale Prediction System (COAMPS) and the Weather Research and Forecasting modeling system in meteorology and the Princeton Ocean Model, the semi-spectral primitive equation model, the s-coordinate Rutgers University model and the Regional Ocean Modeling System in oceanography [10, 15–20]. More precisely, using the chain rule of spatial partial derivatives from the Cartesian coordinate to the σ-coordinate, the scalar equations in the σ-coordinate (the transformed equations) are obtained.

Gal-Chen and Somerville [21] used the second type to obtain scalar equations, when they designed the height-based terrain-following σ_z-coordinate. Expanding the atmospheric vector equations according to the covariant basis vectors of the σ_z-coordinate, they obtained the contravariant scalar equations of the σ_z-coordinate (the expanded equations). Xue et al. [22] used a set of modified equations based on Gal-Chen and Somerville's method in their Advanced Regional Prediction System (ARPS).

2.2 Computational errors of the PGF

The computational errors of the PGF in both existing methods are derived from the same computational forms of the PGF,

$$-\frac{1}{\rho}\left(\frac{\partial p}{\partial x}\right)_z=-\frac{1}{\rho}\left(\frac{\partial p}{\partial x}\right)_\sigma-\frac{1}{\rho}\frac{\partial p}{\partial \sigma}\cdot\frac{\partial \sigma}{\partial x},$$
$$-\frac{1}{\rho}\left(\frac{\partial p}{\partial y}\right)_z=-\frac{1}{\rho}\left(\frac{\partial p}{\partial y}\right)_\sigma-\frac{1}{\rho}\frac{\partial p}{\partial \sigma}\cdot\frac{\partial \sigma}{\partial y},$$

which are no longer one term on the right hand side (RHS) of the equation. While these terms are typically opposite in sign near the upslope and downslope of steep topography, their causes are different in the two types. In the basis equations of most numerical models obtained by the first type, because of the sum of the two terms in the chain rule of spatial partial derivatives,

$$\left(\frac{\partial F}{\partial x}\right)_z=\left(\frac{\partial F}{\partial x}\right)_\sigma+\frac{\partial F}{\partial \sigma}\cdot\left(\frac{\partial \sigma}{\partial x}\right)_z,$$
$$\left(\frac{\partial F}{\partial y}\right)_z=\left(\frac{\partial F}{\partial y}\right)_\sigma+\frac{\partial F}{\partial \sigma}\cdot\left(\frac{\partial \sigma}{\partial y}\right)_z,$$

where F is a scalar, the PGF computational forms in the transformed equations are altered from one term to two. However, in the contravariant scalar equations obtained by Gal-Chen and Somerville [21] using the second type, the PGF computational forms in the expanded equations are due to the expression of scalar gradient in a curvilinear coordinate system, which will be analyzed later.

Since the PGF is calculated through pressure gradient (e.g., $-1/\rho\cdot\nabla p$), when adopting the second type to implement σ-coordinate in a numerical model, the forms of PGF in the expanded equations depend on the expression of a scalar gradient in a curvilinear coordinate. This expression is given by Wang and Xiong [23] as follows,

$$\nabla\phi=\frac{\partial\phi}{\partial x^i}\mathbf{i}_i=\frac{\partial\phi}{\partial q^j}\frac{\partial q^j}{\partial x^i}\mathbf{i}_i=\frac{\partial\phi}{\partial q^j}\mathbf{e}^j=\mathbf{g}^{ij}\frac{\partial\phi}{\partial q^j}\mathbf{e}_i, \tag{2.1}$$

where i and j sum from 1 to 3, ϕ is a scalar, $\mathbf{i}_i$ are the basis vectors of the Cartesian coordinate, $\mathbf{e}^j$ and $\mathbf{e}_i$ are the contravariant and covariant basis vectors of a curvilinear coordinate, respectively, and $\mathbf{g}^{ij}$is the contravariant metric tensor. Explicitly, the terms $\frac{\partial\phi}{\partial q^j}\mathbf{e}^j$ and $\mathbf{g}^{ij}\frac{\partial\phi}{\partial q^j}\mathbf{e}_i$ in Eq. (2.1) manifest that using covariant basis vectors, $\mathbf{e}_i$, the expression of $\nabla\phi$ is a sum of three terms in each direction of $\mathbf{e}_i$($\mathbf{e}_1$, $\mathbf{e}_2$ and $\mathbf{e}_3$); whereas using contravariant basis vectors, $\mathbf{e}^j$, in each of its directions ($\mathbf{e}^1$, $\mathbf{e}^2$ and $\mathbf{e}^3$) the expression of $\nabla\phi$ is only one term. In particular, if every row of $\mathbf{g}^{ij}$(g^{1j}, g^{2j} and g^{3j}) has only one non-zero element, the expression of $\nabla\phi$ can be one term while using the covariant basis vectors. Unfortunately, the contravariant metric tensor $\mathbf{g}^{ij}$ of σ_z-coordinate does not conform, which is exactly the reason why the PGF computational forms have more than one term in Gal-Chen and Somerville's equations.

The above analysis indicates that it is not the σ-coordinate but the way it is implemented that causes the well-known PGF problem. Therefore, to tackle the PGF problem we need to search for a new way to implement σ-coordinate.

3 A new method

The scalar gradient in σ-coordinate is one term in each direction when using the contravariant basis vectors to expand the vector equations. The result is one single term in the computational form of the PGF, namely the covariant scalar equations of σ-coordinate.

3.1 Covariant scalar equations in σ-coordinate

Since σ-coordinate is a non-orthogonal coordinate, the covariant and contravariant scalar equations of such a coordinate are always solved by the tensor method in fluid dynamics. Zdundowski and Bott [24] solved the covariant scalar equations of σ-coordinate in this way with normalized definitions of σ-coordinate, whereas their method was complex and their equations were not the common expressions in numerical modeling. We solve the covariant scalar equations in a simpler way, by using the conventional method for solving equations in a spherical coordinate, which belongs to the second type of method. For simplicity, we assume there is no friction. The classic expressions of σ-coordinate defined by Gal-Chen and Somerville [21] used by many numerical models (such as RAMS, COAMPS, and ARPS) are used in the following computation as an example. Their definitions are as follows,

$$x' = x, \tag{3.1}$$

$$y' = y, \tag{3.2}$$

$$\sigma = H\frac{z-h}{H-h}, \tag{3.3}$$

where x', y', and σ are coordinates of the σ-coordinate, H is the top of the atmosphere in a model and $h=h(x,y)$ represents the terrain.

Expanding each term in the vector equations according to the contravariant basis vectors $\mathbf{e}^i$ of σ-coordinate, we can obtain momentum, mass and heat equations in their covariant scalar forms of the σ-coordinate, respectively. First, we expand the vector form of momentum equations,

$$\frac{\partial \mathbf{v}}{\partial t}+(\mathbf{v}\cdot\boldsymbol{\nabla})\mathbf{v} = -\frac{1}{\rho}\boldsymbol{\nabla} p - 2\boldsymbol{\Omega}\times\mathbf{v}+\mathbf{g}. \tag{3.4}$$

The left hand side (LHS) of Eq. (3.4) is transformed into

$$\frac{\partial \mathbf{v}}{\partial t} = \frac{\partial v_i}{\partial t}\mathbf{e}^i + v_i\frac{\partial \mathbf{e}^i}{\partial t} = \frac{\partial v_i}{\partial t}\mathbf{e}^i,$$

and

$$(\mathbf{v}\cdot\boldsymbol{\nabla})\mathbf{v} = \frac{1}{2}\boldsymbol{\nabla}(\mathbf{v}\cdot\mathbf{v}) - \mathbf{v}\times(\boldsymbol{\nabla}\times\mathbf{v})$$

$$=\frac{1}{2}\frac{\partial v_m v_n g^{mn}}{\partial q^i}\mathbf{e}^i-\mathbf{e}^i\left\{\begin{array}{l}\left[v^2\left(\frac{\partial v_2}{\partial q^1}-\frac{\partial v_1}{\partial q^2}\right)-v^3\left(\frac{\partial v_1}{\partial q^3}-\frac{\partial v_3}{\partial q^1}\right)\right]\\-\left[v^1\left(\frac{\partial v_2}{\partial q^1}-\frac{\partial v_1}{\partial q^2}\right)-v^3\left(\frac{\partial v_3}{\partial q^2}-\frac{\partial v_2}{\partial q^3}\right)\right]\\+\left[v^1\left(\frac{\partial v_1}{\partial q^3}-\frac{\partial v_3}{\partial q^1}\right)-v^2\left(\frac{\partial v_3}{\partial q^2}-\frac{\partial v_2}{\partial q^3}\right)\right]\end{array}\right\};$$

while the RHS of Eq. (3.4) is transformed as follows,

$$-\frac{1}{\rho}\nabla p=-\frac{1}{\rho}\frac{\partial p}{\partial q^i}\mathbf{e}^i,$$

$$-2\boldsymbol{\Omega}\times\mathbf{v}=-2\begin{vmatrix}\mathbf{e}_2\times\mathbf{e}_3 & \mathbf{e}_3\times\mathbf{e}_1 & \mathbf{e}_1\times\mathbf{e}_2\\ \Omega^1 & \Omega^2 & \Omega^3\\ v^1 & v^2 & v^3\end{vmatrix}=-2\sqrt{g}\begin{vmatrix}\mathbf{e}^1 & \mathbf{e}^2 & \mathbf{e}^3\\ \Omega^1 & \Omega^2 & \Omega^3\\ v^1 & v^2 & v^3\end{vmatrix}$$

$$=-2\sqrt{g}\left[\mathbf{e}^1\left(\Omega^2v^3-\Omega^3v^2\right)-\mathbf{e}^2\left(\Omega^1v^3-\Omega^3v^1\right)+\mathbf{e}^3\left(\Omega^1v^2-\Omega^2v^1\right)\right],$$

and $\mathbf{g}=g_i\mathbf{e}^i$. Second, we expand the vector form of mass equation,

$$\frac{\partial\rho}{\partial t}+\nabla\cdot(\rho\mathbf{v})=0. \tag{3.5}$$

Only the second term on the LHS of Eq. (3.5) changes to

$$\nabla\cdot(\rho\mathbf{v})=\frac{1}{\sqrt{g}}\frac{\partial}{\partial q^i}\left(\sqrt{g}\rho v^i\right).$$

Third, the vector form of heat equation is given by

$$\frac{\partial T}{\partial t}+\mathbf{v}\cdot\nabla T-\frac{RT}{C_pp}\frac{dp}{dt}=\frac{Q}{C_p}. \tag{3.6}$$

The second term on the LHS of Eq. (3.6) changes to

$$\mathbf{v}\cdot\nabla T=v^i\frac{\partial T}{\partial q^i}.$$

Now, the covariant equations in σ-coordinate can be solved. The momentum equations are

$$\frac{\partial v_i}{\partial t}\mathbf{e}^i+\frac{1}{2}\frac{\partial v_m v_n g^{mn}}{\partial q^i}\mathbf{e}^i-\mathbf{e}^i\left\{\begin{array}{l}\left[v^2\left(\frac{\partial v_2}{\partial q^1}-\frac{\partial v_1}{\partial q^2}\right)-v^3\left(\frac{\partial v_1}{\partial q^3}-\frac{\partial v_3}{\partial q^1}\right)\right]\\-\left[v^1\left(\frac{\partial v_2}{\partial q^1}-\frac{\partial v_1}{\partial q^2}\right)-v^3\left(\frac{\partial v_3}{\partial q^2}-\frac{\partial v_2}{\partial q^3}\right)\right]\\+\left[v^1\left(\frac{\partial v_1}{\partial q^3}-\frac{\partial v_3}{\partial q^1}\right)-v^2\left(\frac{\partial v_3}{\partial q^2}-\frac{\partial v_2}{\partial q^3}\right)\right]\end{array}\right\}$$

$$=-\frac{1}{\rho}\frac{\partial p}{\partial q^i}\mathbf{e}^i-2\sqrt{g}\left[\mathbf{e}^1\left(\Omega^2v^3-\Omega^3v^2\right)-\mathbf{e}^2\left(\Omega^1v^3-\Omega^3v^1\right)+\mathbf{e}^3\left(\Omega^1v^2-\Omega^2v^1\right)\right]+g_i\mathbf{e}^i; \tag{3.7}$$

or in an explicit form for each direction of $\mathbf{e}^i$ as follows,

$$\frac{\partial v_1}{\partial t}+v^1\frac{\partial v_1}{\partial q^1}+v^2\frac{\partial v_1}{\partial q^2}+v^3\frac{\partial v_1}{\partial q^3}-\frac{1}{2}v^m v^n\frac{\partial g_{mn}}{\partial q^1}=-\frac{1}{\rho}\frac{\partial p}{\partial q^1}-2\sqrt{g}\left(\Omega^2 v^3-\Omega^3 v^2\right)+g_1, \tag{3.8}$$

$$\frac{\partial v_2}{\partial t}+v^1\frac{\partial v_2}{\partial q^1}+v^2\frac{\partial v_2}{\partial q^2}+v^3\frac{\partial v_2}{\partial q^3}-\frac{1}{2}v^m v^n\frac{\partial g_{mn}}{\partial q^2}=-\frac{1}{\rho}\frac{\partial p}{\partial q^2}+2\sqrt{g}\left(\Omega^1 v^3-\Omega^3 v^1\right)+g_2, \tag{3.9}$$

$$\frac{\partial v_3}{\partial t}+v^1\frac{\partial v_3}{\partial q^1}+v^2\frac{\partial v_3}{\partial q^2}+v^3\frac{\partial v_3}{\partial q^3}-\frac{1}{2}v^m v^n\frac{\partial g_{mn}}{\partial q^3}=-\frac{1}{\rho}\frac{\partial p}{\partial q^3}-2\sqrt{g}\left(\Omega^1 v^2-\Omega^2 v^1\right)+g_3. \tag{3.10}$$

The mass equation is written as

$$\frac{\partial \rho}{\partial t}+\frac{1}{\sqrt{g}}\frac{\partial}{\partial q^i}\left(\sqrt{g}\rho v^i\right)=0; \tag{3.11}$$

the heat equation,

$$\frac{\partial T}{\partial t}+v^i\frac{\partial T}{\partial q^i}-\frac{RT}{C_p p}\frac{dp}{dt}=\frac{Q}{C_p}; \tag{3.12}$$

and the equation of state,

$$p=\rho RT. \tag{3.13}$$

In Eqs. (3.7)-(3.13), m, n and i sum from 1 to 3, q^i is the new σ-coordinate, superscript represents contravariant variables, and subscript is for covariant variables. Variables g_{mn} and g^{mn} are the components of the covariant and contravariant metric tensors, and $\sqrt{g}$ is the functional determinate of the system. These three variables are related to the coordinate definitions, with the expressions in σ_z-coordinate giving by

$$\mathbf{g}_{mn}=\begin{pmatrix} 1+\left(1-\frac{q^3}{H}\right)^2\left(\frac{\partial h}{\partial q^1}\right)^2 & \left(1-\frac{q^3}{H}\right)^2\frac{\partial h}{\partial q^1}\frac{\partial h}{\partial q^2} & \left(1-\frac{q^3}{H}\right)\cdot\frac{\partial h}{\partial q^1}\cdot\frac{H-h}{H} \\ \left(1-\frac{q^3}{H}\right)^2\frac{\partial h}{\partial q^1}\frac{\partial h}{\partial q^2} & 1+\left(1-\frac{q^3}{H}\right)^2\left(\frac{\partial h}{\partial q^2}\right)^2 & \left(1-\frac{q^3}{H}\right)\cdot\frac{\partial h}{\partial q^2}\cdot\frac{H-h}{H} \\ \left(1-\frac{q^3}{H}\right)\cdot\frac{\partial h}{\partial q^1}\cdot\frac{H-h}{H} & \left(1-\frac{q^3}{H}\right)\cdot\frac{\partial h}{\partial q^2}\cdot\frac{H-h}{H} & \left(\frac{H-h}{H}\right)^2 \end{pmatrix},$$

$$\mathbf{g}^{mn}=\begin{pmatrix} 1 & 0 & \frac{H(z-H)}{(H-h)^2}\frac{\partial h}{\partial x} \\ 0 & 1 & \frac{H(z-H)}{(H-h)^2}\frac{\partial h}{\partial y} \\ \frac{H(z-H)}{(H-h)^2}\frac{\partial h}{\partial x} & \frac{H(z-H)}{(H-h)^2}\frac{\partial h}{\partial y} & \frac{H^2}{(H-h)^2}\left[\frac{(z-H)^2}{(H-h)^2}\left(\frac{\partial h}{\partial x}\right)^2+\frac{(z-H)^2}{(H-h)^2}\left(\frac{\partial h}{\partial y}\right)^2+1\right] \end{pmatrix},$$

Table 1: Comparison of three methods to implement σ-coordinate in numerical models.

Method type	description	Coordinate of scaler equations	Computational forms of PGF
first type	- using the chain rule from the Cartesian coordinate to σ-coordinate	- the Cartesian coordinate	- sum of two terms in horizontal and vertical momentum equations
second type	- using the *covariant* basis vectors of σ-coordinate to obtain the *contravariant* scalar equations	- the non-orthogonal curvilinear σ-coordinate	- sum of two terms in horizontal momentum equations; sum of three terms in vertical momentum equation
	- using the *contravariant* basis vectors of σ-coordinate to obtain the *covariant* scalar equations	- the non-orthogonal curvilinear σ-coordinate	- one term in horizontal and vertical momentum equations

Table 2: Main characteristics of covariant equations in σ-coordinate and their causes.

Main characteristics	Causes
- the computational form of PGF is one term in each momentum equation	- using contravariant basis vectors $\mathbf{e}^j$
- $\sqrt{g}$ and curvature term in every momentum equation	- non-orthogonal and curvilinear characteristics of σ-coordinate
- a gravity term g_i in every momentum equation	- contravariant basis vectors $\mathbf{e}^3$ is not vertical
- vectors should be decomposed according to basis vector $\mathbf{e}_i$ or $\mathbf{e}^j$	- using the second type to obtain the scalar equations in σ-coordinate

and

$$\sqrt{g}=\sqrt{|\mathbf{g}_{mn}|}=\frac{H-h}{H}.$$

The first term on the RHS of each of the Eq. (3.8)-(3.10) is the PGF expression, which is one single term in each equation. Actually, unlike the equations obtained by the first type method, the Eqs. (3.8)-(3.13) are expressed in the non-orthogonal curvilinear σ-coordinate and the contravariant basis vectors ensure the simple forms of PGF. Comparing the three methods of implementing σ-coordinate in numerical models (Table 1) allows us to elucidate that only by using contravariant basis vectors of σ-coordinate to expand atmospheric vector equations into the covariant scalar equations will the expression of the PGF result in one single term in each of the three momentum equations.

Characteristics of the covariant equations in σ-coordinate are summarized in Table 2. Concerning the third characteristic, the negative horizontal PGF (HPGF) which is opposite in sign with the components of gravity in Eqs. (3.8) and (3.9) may bring new compu-

tational errors, however the HPGF is much less than the corresponding components of gravity thereby avoiding the potential problem. With regard to the fourth characteristic, decomposing a vector in σ-coordinate is the same matter as knowing a certain vector's components in the Cartesian coordinate to obtain its components in σ-coordinate. So, let the expressions of a vector $\mathbf{A}$ in the Cartesian coordinate and σ-coordinate be

$$\mathbf{A}=a\mathbf{i}+b\mathbf{j}+c\mathbf{k}, \tag{3.14}$$

$$\mathbf{A}=\alpha'\mathbf{e}_1+\beta'\mathbf{e}_2+\gamma'\mathbf{e}_3, \tag{3.15}$$

$$\mathbf{A}=\alpha\mathbf{e}^1+\beta\mathbf{e}^2+\gamma\mathbf{e}^3, \tag{3.16}$$

respectively. Then, we substitute the expressions of covariant and contravariant basis vectors of σ_z-coordinate,

$$\mathbf{e}_1=\mathbf{i}+\left[\left(1-\frac{q^3}{H}\right)\frac{\partial h}{\partial q^1}\right]\cdot\mathbf{k},\qquad \mathbf{e}_2=\mathbf{j}+\left[\left(1-\frac{q^3}{H}\right)\frac{\partial h}{\partial q^2}\right]\cdot\mathbf{k},\qquad \mathbf{e}_3=\left(\frac{H-h}{H}\right)\cdot\mathbf{k},$$

$$\mathbf{e}^1=\mathbf{i},\qquad \mathbf{e}^2=\mathbf{j},\qquad \mathbf{e}^3=\left[\frac{H(z-H)}{(H-h)^2}\frac{\partial h}{\partial x}\right]\mathbf{i}+\left[\frac{H(z-H)}{(H-h)^2}\frac{\partial h}{\partial y}\right]\mathbf{j}+\left(\frac{H}{H-h}\right)\mathbf{k},$$

in Eqs. (3.15) and (3.16) to obtain

$$\mathbf{A}=\alpha'\left[\mathbf{i}+\left(1-\frac{q^3}{H}\right)\frac{\partial h}{\partial q^1}\cdot\mathbf{k}\right]+\beta'\left[\mathbf{j}+\left(1-\frac{q^3}{H}\right)\frac{\partial h}{\partial q^2}\cdot\mathbf{k}\right]+\gamma'\left(\frac{H-h}{H}\cdot\mathbf{k}\right), \tag{3.17}$$

$$\mathbf{A}=\alpha\mathbf{i}+\beta\mathbf{j}+\gamma\left\{\left[\frac{H(z-H)}{(H-h)^2}\frac{\partial h}{\partial x}\right]\mathbf{i}+\left[\frac{H(z-H)}{(H-h)^2}\frac{\partial h}{\partial y}\right]\mathbf{j}+\left(\frac{H}{H-h}\right)\mathbf{k}\right\}. \tag{3.18}$$

Comparing (3.14) to (3.17) and (3.18), we can solve

$$\alpha'=a,\qquad \beta'=b,\qquad \gamma'=\frac{c-a\left(1-\frac{q^3}{H}\right)\frac{\partial h}{\partial q^1}-b\left(1-\frac{q^3}{H}\right)\frac{\partial h}{\partial q^2}}{\frac{H-h}{H}},$$

$$\alpha=a+c\frac{H-z}{H-h}\frac{\partial h}{\partial x},\qquad \beta=b+c\frac{H-z}{H-h}\frac{\partial h}{\partial y},\qquad \gamma=c\frac{H-h}{H}.$$

Then, the expressions of vector $\mathbf{A}$ in σ_z-coordinate become

$$\mathbf{A}=\alpha'\mathbf{e}_1+\beta'\mathbf{e}_2+\gamma'\mathbf{e}_3=a\mathbf{e}_1+b\mathbf{e}_2+\left[\frac{c-a\left(1-\frac{q^3}{H}\right)\frac{\partial h}{\partial q^1}-b\left(1-\frac{q^3}{H}\right)\frac{\partial h}{\partial q^2}}{\frac{H-h}{H}}\right]\mathbf{e}_3, \tag{3.19}$$

$$\mathbf{A}=\alpha\mathbf{e}^1+\beta\mathbf{e}^2+\gamma\mathbf{e}^3=\left(a+c\frac{H-z}{H-h}\frac{\partial h}{\partial x}\right)\mathbf{e}^1+\left(b+c\frac{H-z}{H-h}\frac{\partial h}{\partial y}\right)\mathbf{e}^2+\left(c\frac{H-h}{H}\right)\mathbf{e}^3. \tag{3.20}$$

Note that the two horizontal contravariant components of vector $\mathbf{A}$ in σ_z-coordinate are the same as those in the Cartesian coordinate, but the others are different.

3.2 Using covariant equations of σ-coordinate in a numerical model

Based on the characteristics of the covariant scalar equations listed in Table 2, we can conveniently implement the equations in a numerical model by setting corresponding parameters in the scalar equations of the Cartesian coordinate.

Define the parameters λ_{11}, λ_{12}, λ_{13} and λ_2 as

$$\lambda_{11}=-\frac{1}{2}v^m v^n\frac{\partial g_{mn}}{\partial q^1},\qquad \lambda_{12}=-\frac{1}{2}v^m v^n\frac{\partial g_{mn}}{\partial q^2},$$
$$\lambda_{13}=-\frac{1}{2}v^m v^n\frac{\partial g_{mn}}{\partial q^3},\qquad \lambda_2=\sqrt{g}.$$

Then Eqs. (3.8)-(3.13) can be re-written as

$$\frac{\partial v_1}{\partial t}+v^1\frac{\partial v_1}{\partial q^1}+v^2\frac{\partial v_1}{\partial q^2}+v^3\frac{\partial v_1}{\partial q^3}+\lambda_{11}=-\frac{1}{\rho}\frac{\partial p}{\partial q^1}-2\lambda_2\left(\Omega^2v^3-\Omega^3v^2\right)+g_1, \tag{3.21}$$
$$\frac{\partial v_2}{\partial t}+v^1\frac{\partial v_2}{\partial q^1}+v^2\frac{\partial v_2}{\partial q^2}+v^3\frac{\partial v_2}{\partial q^3}+\lambda_{12}=-\frac{1}{\rho}\frac{\partial p}{\partial q^2}+2\lambda_2\left(\Omega^1v^3-\Omega^3v^1\right)+g_2, \tag{3.22}$$
$$\frac{\partial v_3}{\partial t}+v^1\frac{\partial v_3}{\partial q^1}+v^2\frac{\partial v_3}{\partial q^2}+v^3\frac{\partial v_3}{\partial q^3}+\lambda_{13}=-\frac{1}{\rho}\frac{\partial p}{\partial q^3}-2\lambda_2\left(\Omega^1v^2-\Omega^2v^1\right)+g_3, \tag{3.23}$$
$$\frac{\partial \rho}{\partial t}+\frac{1}{\lambda_2}\frac{\partial}{\partial q^i}\left(\lambda_2\rho v^i\right)=0, \tag{3.24}$$
$$\frac{\partial T}{\partial t}+v^i\frac{\partial T}{\partial q^i}-\frac{RT}{C_p p}\frac{dp}{dt}=\frac{Q}{C_p}, \tag{3.25}$$
$$p=\rho RT, \tag{3.26}$$

where the expressions of Ω^i and g_i ($i=1$, 2, and 3) are solved in the attached appendix. Through defining different values of these four parameters in σ_z-coordinate and the Cartesian coordinate (Table 3), we can obtain the equations in these two coordinates respectively. In another word, the equations can be directly transformed from the Cartesian

Table 3: Values of the four parameters in the Cartesian coordinate and σ_z-coordinate.

Different parameters	Values	
	in Cartesian coordinate	in σ_z-coordinate
λ_{1i} (represent curvature terms $-\frac{1}{2}v^m v^n\frac{\partial g_{nm}}{\partial q^i}$)	$\lambda_{11}=0$	$\lambda_{11}=-\frac{1}{2}v^m v^n\frac{\partial g_{mn}}{\partial q^1}$
	$\lambda_{12}=0$	$\lambda_{12}=-\frac{1}{2}v^m v^n\frac{\partial g_{mn}}{\partial q^2}$
	$\lambda_{13}=0$	$\lambda_{13}=-\frac{1}{2}v^m v^n\frac{\partial g_{mn}}{\partial q^3}$
λ_2 (represent $\sqrt{g}$)	$\lambda_2=1$	$\lambda_2=\frac{H-h}{H}$

coordinate to σ_z-coordinate in a unified framework, and vice versa. Note that in order to satisfy the boundary condition of vertical velocity, the covariant velocities should be transformed into their contravariant forms, as $v^i = v_m g^{mi}$ given by Zdundowski and Bott [24].

Actually, those terms converted to the four parameters are all related to the coordinate definitions of σ-coordinate, and so will automatically change their values in the horizontal as defined in Table 3. However, there are some additional advantages of such a definition besides the convenience: 1) identifying the terms related to coordinate systems, 2) representing the effects of terrain, and 3) profiting in using the σ-z hybrid coordinate in the vertical via defining those four parameters as in Table 3 respectively for the upper and lower areas of a fixed transition level.

4 Idealized experiments of calculating the PGF

In order to find out whether the new method could calculate the PGF more accurately, the experiments upon two kinds of idealized pressure fields in the vertical are carried out. The one is without horizontal gradient, and the other is with both horizontal and vertical gradient. Considering to calculate the PGF in the x-direction as an example, the space discretization of the PGF terms in the classic and new methods upon leapfrog scheme in the horizontal and forward scheme in the vertical are listed as follows respectively, in the classic method,

$$\frac{\partial p_{i,k}}{\partial x} = \frac{p_{i+1,k} - p_{i-1,k}}{2\Delta x} - \frac{p_{i,k+1} - p_{i,k}}{\Delta z} \cdot \left(\frac{\partial z}{\partial x}\right)_\sigma, \tag{4.1}$$

in the new method,

$$\left(\frac{\partial p_{i,k}}{\partial x}\right)_\sigma = \frac{p_{i+1,k} - p_{i-1,k}}{2\Delta x}. \tag{4.2}$$

The classic definitions of σ-coordinate, Eqs. (3.1)-(3.3), are still used in the two experiments. The bell-shaped terrain is adopted, the definition of which is given by,

$$h(x) = \overline{H} \cdot \frac{a^2}{(x - h_0)^2 + a^2},$$

where $\overline{H}$ is the maximum height of the terrain, a is the half-width, and h_0 is the middle point of the terrain. Here, we choose $\overline{H} = 4$ km, $a = 5$ km, and $h_0 = 50$ km. Domain of the experiments is 37 km in the vertical and 100 km in the horizontal. We choose $\Delta x = 5000$m and $\Delta z = 3700$m obtaining 21 grids in the horizontal and 10 levels in the vertical.

4.1 No horizontal PGF experiment

Because of the different "horizontal directions" in the classic and the new methods, we designed two pressure fields with their definitions given by, in the classic method,

$$p = p_0 \cdot e^{\left(-\frac{z}{\lambda}\right)}, \tag{4.3}$$

in the new method,

$$p = p_0 \cdot e^{\left(-\frac{\sigma}{\lambda}\right)}. \tag{4.4}$$

where p_0 is the surface pressure and λ is the scale height of atmosphere. Via Eqs. (4.3)-(4.4), we obtain

$$\left(\frac{\partial p}{\partial x}\right)_z = 0, \tag{4.5}$$

$$\left(\frac{\partial p}{\partial x}\right)_\sigma = 0. \tag{4.6}$$

The Eqs. (4.5)-(4.6) manifest that there are no horizontal PGF in both methods. In another word, the analytic values of PGF in both methods are zero.

Here, we choose $p_0 = 1015.0$ hPa and $\lambda = 8$ km in Eqs. (4.3)-(4.4), so as to obtain the pressure on the top height is 10 hPa which is common in many numerical models. The pressure fields given by Eqs. (4.3)-(4.4) are similar to that of the real atmosphere (Fig. 2).

We calculate the PGF by Eqs. (4.1)-(4.2) to solve the numerical value of PGF (PGFn) in both methods respectively. The PGFn subtracted from the analytic value of PGF (PGFa) on every grids are the absolute error (AE) illustrated in Fig. 3. In the whole domain, AE in the new method (Fig. 3(b)) is reduced by more than five orders of magnitude compared with the AE obtained by the classic method (Fig. 3(a)), and the maximal AE in the new method is practically zero. Moreover, unlike the AE pattern in the classic method which has symmetrical maxima on the slope of terrain, the AE pattern of the new method exhibits little correlation with terrain, indicating that the PGF calculated by the new method is almost independent of the terrain.

4.2 With horizontal PGF experiment

We designed a pressure field with non-zero horizontal PGF in both methods, whose definition is given by

$$p = p_0 \cdot e^{\left(-H\frac{z-h}{H-h}\cdot\frac{1}{\lambda}\right)}, \tag{4.7}$$

Here, we choose $\overline{H}$ = 300 m in the function $h = h(x)$and the pressure field is illustrated in Fig. 4.

First, using the Eq. (4.7), we solve the analytic PGF $(\partial p/\partial x)_z$ and $(\partial p/\partial x)_\sigma$respectively, in the classic method,

$$\left(\frac{\partial p}{\partial x}\right)_z = -p_0 \cdot e^{\left(-H\frac{z-h}{H-h}\cdot\frac{1}{\lambda}\right)} \cdot \frac{H}{\lambda} \cdot \frac{z-H}{(H-h)^2}\frac{dh}{dx}, \tag{4.8}$$

in the new method,

$$\left(\frac{\partial p}{\partial x}\right)_\sigma = -p_0 \cdot e^{\left(-H\frac{z-h}{H-h}\cdot\frac{1}{\lambda}\right)} \cdot \frac{H}{\lambda} \cdot \frac{\left(\frac{\partial z}{\partial x}\right)_\sigma (H-h) + \frac{dh}{dx}(z-H)}{(H-h)^2}. \tag{4.9}$$

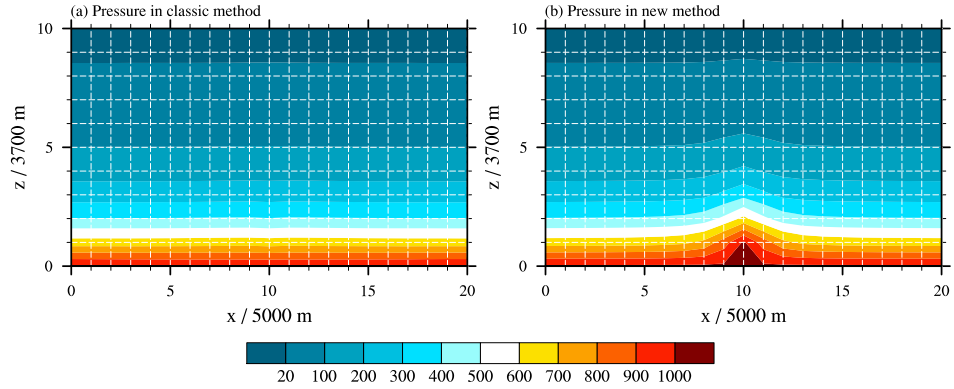

Figure 2: Two pressure fields in the no PGF experiment. The pressure scale (color bar at bottom of figure) is in units of hPa.

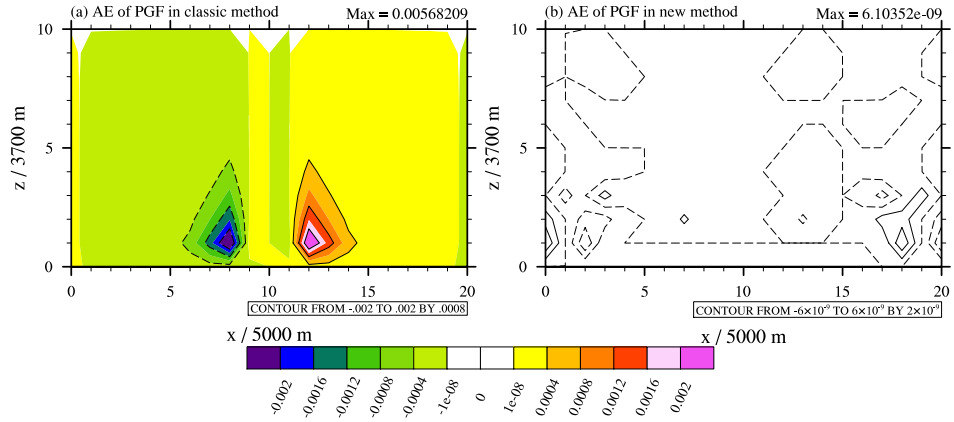

Figure 3: The absolute error of PGF in the classic and new methods. The negative contours are dashed and the spacing intervals of contours in the left and right figure are 0.0008 hPa and 2×10^{-9} hPa respectively. The pressure scale (color bar at bottom of figure) is in units of hPa.

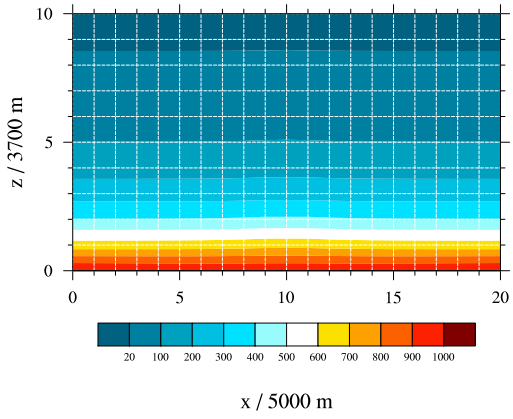

Figure 4: As in Fig. 2 but the pressure field in the experiment of with horizontal PGF.

The analytic PGF obtained by Eqs. (4.8)-(4.9) are illustrated in Figs. 5(a) and 5(b) respectively. Their spatial patterns are similar which have symmetrical maxima on the slope of terrain, but opposite in sign; the PGFa in new method is more than an order of magnitude compared with that in the classic method.

Figs. 5(c) and 5(d) illustrate the numerical PGF calculated by both methods respectively. The PGFn pattern in the new method is more consistent with its PGFa pattern than using the classic method. Specifically, the PGFn pattern of the new method (Fig. 5(d)) remain as the PGFa pattern showed in Fig. 5(b), while the PGFn pattern obtained with the classic method splits into four centers (Fig. 5(c)) even with its main centers (near 8th and 12th grids in x-direction) having the opposite sign compared with PGFa showed in Fig. 5(a).

Second, we calculate the absolute error and the relative error (RE) in both methods (Fig. 6). Although, the maximal AE in the new method is larger than that in the classic method, it exhibits smaller spatial extent than the AE in the classic method (Figs. 6(a) and 6(b)). Furthermore, in the whole domain, the RE of the new method is reduced by an order of magnitude compared with that in the classic method, particularly near the terrain (Figs. 6(c) and 6(d)).

Finally, we calculate the root mean square of AE and RE (RMSE-a and RMSE-r) in the two methods (Table 4). Because the PGFa in the new method is more than an order of magnitude compared with that in the classic method (Fig. 6(a) and 6(b)), the RE is more reasonable for the comparison. The RMSE-r of the new method is reduced by an order of magnitude compared with the result obtained by the classic method, although the RMSE-a of the new method is larger than it in the classic method.

Table 4: The root mean square of AE and RE of PGF in the two methods.

Method to calculate the PGF	Root mean square	
	Absolute error	Relative error
Classic method	0.69×10^{-3}	3.30
New method	1.03×10^{-3}	0.17

5 Summary

The methods of using σ-coordinate in a numerical model are analyzed to illustrate the causes of the well-known PGF problem. Specifically, the PGF problem in σ-coordinate is classified into two types according to their causes. Using the first type to implement σ-coordinate, the PGF problem is caused by the expressions of spatial partial derivative transformations, whose forms are a sum of two terms. Using the second type, the form of scalar gradient expressed by the covariant basis vectors of σ-coordinate is the cause. Note that these two types of PGF problem based on different causes are not the same as "SEFK" and "SESK" proposed by Mellor et al. [25], which were based on different phenomena. In conclusion, the PGF computational error in σ-coordinate is not the result of

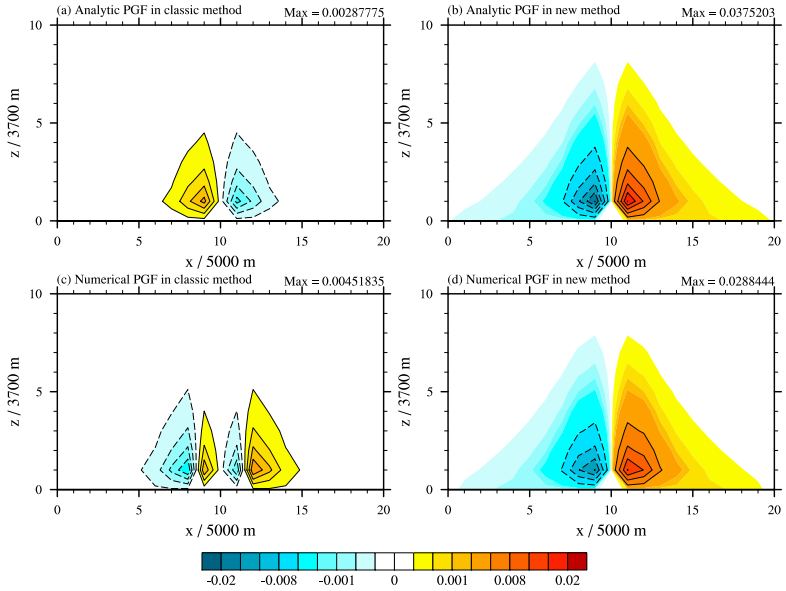

Figure 5: As in Fig. 3 but the analytic and the numerical PGF calculated by the two methods. And the spacing intervals of contours in the left and right figure are 0.0004 hPa and 0.004 hPa respectively.

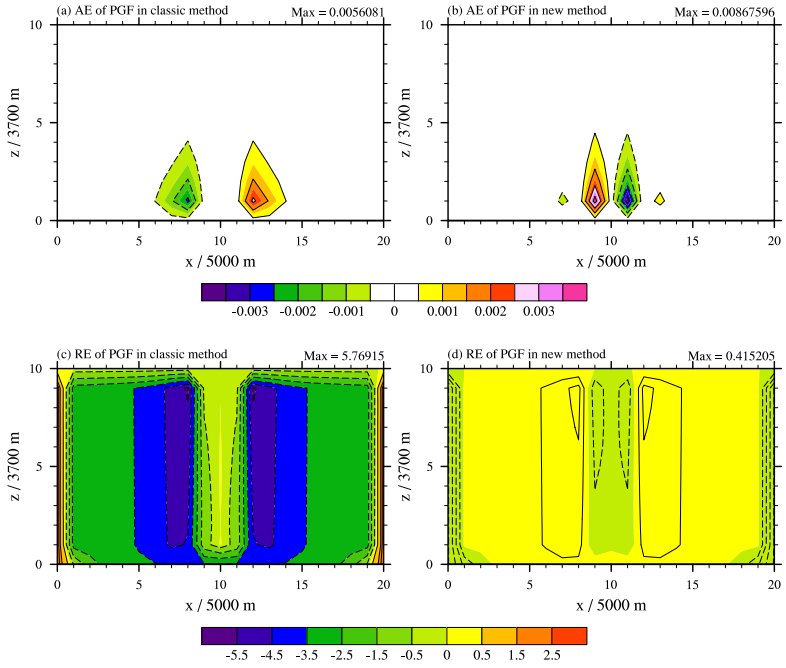

Figure 6: The absolute error and the relative error of PGF in the two methods. The negative contours are dashed. The spacing intervals of contours in (a) and (b) are both 0.001 hPa, while those in (c) and (d) are 1 and 0.1 respectively. The pressure scale (color bar in the middle of figure) is in units of hPa and the color bar at the bottom shows the scale for the relative error.

using σ-coordinate itself, but that of the methods implementing it in a numerical model. The idealized experiments manifest that the PGF expressed in one term can significantly induce less error than the classic sigma method which has the PGF in two terms. Our new way of implementing covariant scalar equations in σ-coordinate via Eqs. (3.21)-(3.26) is not the same as those in previous studies, but convenient with additional advantages.

As in the covariant equations of σ-coordinate solved by Gal-Chen and Somerville [21] and the frequently used equations of spherical coordinate, the curvature terms are included in our Eqs. (3.21)-(3.23) due to the characteristics of covariant metric tensor $\mathbf{g}_{mn}$ of σ-coordinate when using the second type to obtain the covariant equations. These curvature terms may potentially cause numerical problems of a different kind, which needs to be investigated via future numerical experiments. While considering friction in a model, one more parameter defined as the four ones in Table 3 will be required. Incidentally, if the contravariant metric tensor $\mathbf{g}^{mn}$ of a certain terrain-following coordinate conforms to the rule mentioned earlier, namely only one non-zero element in each row of $\mathbf{g}^{mn}$, the PGF computational form will be one term, whether using the covariant basis vectors or the contravariant ones of that coordinate. Therefore, we can choose the covariant or contravariant scalar equations of the coordinate based on some specific requirements.

Since the PGF problem exists in both atmospheric and oceanic models using σ-coordinate, our new method should also apply to numerical ocean models, potentially representing the dynamic effects of terrain more precisely and therefore simulating more realistic circulations in these models. Moreover, the new method proposed in this paper is only theoretical so far, and needs to be validated by more idealized and real-case experiments.

Acknowledgments

We are grateful for all the constructive and detailed comments of the two reviewers. The first and third authors were supported by the Knowledge Innovation Program of the Chinese Academy of Sciences (KZCX2-YW-Q11-04) and the National Basic Research Program of China (973 Program, Grant No. 2011CB309704). The second author was supported by the National Natural Science Foundation of China (NSFC) under Grant No. 40875022, 41175064 and 40633016.

Appendix

The Ω^i and g_i in Eqs. (3.21)-(3.23) can be solved via the Eqs. (3.19)-(3.20) respectively. The expressions of vector $\mathbf{\Omega}$ and $\mathbf{g}$ in the Cartesian coordinate are

$$\mathbf{\Omega} = \Omega\cos\varphi\mathbf{j} + \Omega\sin\varphi\mathbf{k},$$
$$\mathbf{g} = -g\mathbf{k}.$$

Substitute the corresponding components of $\mathbf{\Omega}$ and $\mathbf{g}$ into Eqs. (3.19)-(3.20) respectively, we can obtain

$$\Omega^1=0,\qquad \Omega^2=\Omega\cos\varphi,\qquad \Omega^3=\frac{\Omega\sin\varphi-\Omega\cos\varphi\left(1-\frac{\sigma}{H}\right)\frac{\partial h}{\partial y}}{\frac{H-h}{H}};$$

$$g_1=-g\frac{H-z}{H-h}\frac{\partial h}{\partial x},\qquad g_2=-g\frac{H-z}{H-h}\frac{\partial h}{\partial y},\qquad g_3=-g\frac{H-h}{H}.$$

References

[1] N. A. Phillips, A coordinate system having some special advantages for numerical forecasting, J. Meteorol., 14 (1957), 184-185.

[2] M. Danard, Q. Zhang and J. Kozlowski, On computing the horizontal pressure gradient force in sigma coordinates, Mon. Weather Rev., 121 (1993), 3173-3183.

[3] J. Berntsen and L.-Y. Oey, Estimation of the internal pressure gradient in σ-coordinate ocean models: Comparison of second-, fourth-, and sixth-order schemes, Ocean Dyn., 60 (2010), 317-330.

[4] J. Smagorinsky, R. F. Strickler, W. E. Sangster, S. Manabe, J. L. Halloway Jr. and G. D. Hembree, Prediction experiments with a general circulation model. Proc. Int. Symp. on Dynamics of Large Scale Atmospheric Processes, Moscow, USSR, 70-134, 1967.

[5] J. Steppeler, R. Hess, U. Schättler and L. Bonaventura, Review of numerical methods for nonhydrostatic weather prediction models, Meteorol. Atmos. Phys., 82 (2003), 287-301.

[6] J. Hu and P. Wang, The errors of pressure gradient force in high-resolution mesoscale model with terrain-following coordinate and its revised scheme (in Chinese), Chin. J. Atoms. Sci., 31 (2007), 109-118.

[7] G. A. Corby, A. Gilchrist and R. L. Newson, A general circulation model of the atmosphere suitable for long period integrations, Q. J. R. Meteorol. Soc., 98 (1972), 809-832.

[8] J. M. Gary, Estimate of truncation error in transformed coordinate, primitive equation atmospheric models, J. Atmos. Sci., 30 (1973), 223-233.

[9] Y. Qian and Z. Zhong, General forms of dynamic equations for atmosphere in numerical models with topography, Adv. Atmos. Sci., 3 (1986), 10-22.

[10] A. F. Blumberg and G. L. Mellor, A description of a three-dimensional coastal ocean circulation model. Three-dimensional coastal ocean models, N. S. Heaps, Ed., American Geophysical Union, 1987.

[11] J. D. McCalpin, A comparison of second-order and fourth-order pressure gradient algorithms in a sigma coordinate ocean model, Int. J. Numer. Methods Fluids., 18 (1994), 361-383.

[12] X. Yang and Y. Qian, The recurrent computational methods of pressure gradient force in the p-σ coordinate numerical models (in Chinese), Chin. J. Atmos. Sci., 27 (2003), 171-181.

[13] M. D. Sikirić, I. Janeković and M. Kuzmić, A new approach to bathymetry smoothing in σ-coordinate ocean models, Ocean Modell., 29 (2009), 128-136.

[14] J. Berntsen, A perfectly balanced method for estimating the internal pressure gradients in σ-coordinate ocean models, Ocean Modell., 38 (2011), 85-95.

[15] R. A. Pielke, W. R. Cotton, R. L. Walko, C. J. Tremback, W. A. Lyons, L. D. Grasso, M. E. Nicholls, M. D. Moran, D. A. Wesley, T. J. Lee and J. H. Copeland, A comprehensive meteorological modeling system-RAMS, Meteorol. Atmos. Phys., 49 (1992), 69-91.

[16] R. M. Hodur, The naval research laboratory's coupled ocean/atmosphere mesoscale prediction system (COAMPS), Mon. Weather Rev., 125 (1997), 1414-1430.
[17] J. Dudhia, cited 2011: WRF modeling system overview. `http://www.mmm.ucar.edu/wrf/users/tutorial/201001/WRF_Overview_Dudhia.pdf`
[18] D. B. Haidvogel, J. L. Wilkin and R. Young, A semi-spectral primitive equation ocean circulation model using vertical sigma and orthogonal curvilinear horizontal coordinate, J. Comput. Phys., 94 (1991), 151-185.
[19] Y. Song and D. Haidvogel, A semi-implicit ocean circulation model using a generalized topography-following coordinate system, J. Comput. Phys., 115 (1994), 228-248.
[20] D. B. Haidvogel, H. G. Arango, K. Hedstrom, A. Beckmann, P. Malanotte-Rizzoli and A. F. Shchepetkin, Model evaluation experiments in the north atlantic basin: Simulations in nonlinear terrain-following coordinates, Dyn. Atmos. Oceans., 32 (2000), 239-281.
[21] T. Gal-Chen and R. C. J. Somerville, On the use of a coordinate transformation for the solution of the Navier-stokes equations, J. Comput. Phys., 17 (1975), 209-228.
[22] M. Xue, K. K. Droegemeier and V. Wong, The advanced regional prediction system (ARPS) – a multi-scale nonhydrostatic atmospheric simulation and prediction model. Part I: Model dynamics and verification, Meteorol. Atmos. Phys., 75 (2000), 161-193.
[23] X. Wang and A. Xiong, Advanced Fluid Dynamics (in Chinese), Huazhong University of Science and Technology Press, 2003.
[24] W. Zdunkowski and A. Bott, Dynamics of the Atmosphere: A Course in Theoretical Meteorology, Cambridge University Press, 2003.
[25] G. L. Mellor, L.-Y. Oey and T. Ezer, Sigma coordinate pressure gradient errors and the seamount problem, J. Atmos. Oceanic Technol., 15 (1998), 1122-1131.